
**DYNAMIC POSITIONING CONFERENCE**
**November 15-16, 2005**

## Control Systems I

# Nonlinear Observer Design for Dynamic Positioning

**J.G. Snijders, J.W. van der Woude**
***Delft University of Technology (The Netherlands)***

**J. Westhuis**
***Gusto BV (The Netherlands)***

**Abstract**

Recent developments in optimal observer design for dynamic positioning have led to application of contraction analysis. In this paper a theoretical method for nonlinear optimal observer design and a suboptimal observer using a state-dependent Riccati equation approach are presented. The observer will be compared to an existing observer and its properties and performance is discussed. Early observer design for dynamic positioning (DP) focussed on applying linear optimal observer theory to the linearized equations of motion. Because of the large number of free parameters and the lack of global stability, the research area shifted to nonlinear observer design. The drawback of this approach however is that optimality is not guaranteed. Based on recent developments in the field of contraction theory a theoretical optimal nonlinear observer is presented, yielding, together with a state-dependent Riccati equation approach, a suboptimal observer design. Performance and applicability of this new observer are compared to an existing observer.

**Keywords**

Nonlinear observer, contraction theory, dynamic positioning, state-dependent Riccati equations

## 1 Introduction

The total vessel motion can be modeled as the superposition of the low-frequency (LF) vessel motions and the wave-frequency (WF) motions. For dynamic positioning purposes it is important to obtain accurate estimates of the LF motions from the noisy position and heading measurements such that only these motions are used for station keeping. This is referred to as state estimation and wave filtering. The first wave filtering methods were developed in the 1970's. They were extended and modified in the years thereafter. In these methods the wave filtering and state estimation problems were solved using linear Kalman filters [3]. A major drawback of these Kalman filter-based estimators is the necessity of linearization about a set of pre-defined yaw angles because of which global stability can not be guaranteed and the performance of the estimator is degraded. In addition to the fact that tuning the free parameters of the Kalman filter is time consuming, in [4, 10, 12] the possibilities of nonlinear observer design were considered. These nonlinear observer designs are proved to be stable but optimality is not yet examined. In this paper a nonlinear optimal observer in general form is presented and an observer design method using state-dependent Riccati equation techniques is introduced. Performance and applicability of this new observer is compared to an existing observer.
In the first section the mathematical model to describe the dynamic vessel motions as presented in [4, 10] is summarized, in the second section the nonlinear observer is derived as in [7] and the suboptimal observer of [1] is presented. Thereafter, for the specific model of [4, 10] simulation results are presented comparing the new observer and an existing observer, and conclusions are drawn.

## 2 Mathematical model

One of the objectives of this paper is a comparision of the performance of a SDRE observer as in [1] to the observer obtained in [4]. In order to be able to compare the two designs the mathematical model presented in [4] is used. In this model the total ship motion is considered to be the superposition of LF and WF motions. In this section this model will briefly be reviewed.

## 2.1 Kinematic equations of motion

For the presentation of the motion of marine vehicles the introduction of two coordinate systems is convenient. A moving coordinate system $XYZ$ is fixed to the vessel and called the body-fixed frame. Its origin $O$ is normally chosen to coinside with the center of gravity of the vessel. The motion of the body-fixed frame is described relative to an earth-fixed frame $X_E Y_E Z_E$. The position $(x, y)$ and heading $\psi$ of the vessel relative to the earth-fixed frame can now be expressed in vector form by $\boldsymbol{\eta} = \begin{bmatrix} x & y & \psi \end{bmatrix}^T$. Decomposing the velocities in a vessel-fixed frame yields the vector $\boldsymbol{\nu} = \begin{bmatrix} u & v & r \end{bmatrix}^T$. The relation between the vessel-fixed and earth-fixed frame can be expressed by the tranformation

$$\dot{\boldsymbol{\eta}} = J(\boldsymbol{\eta})\boldsymbol{\nu}$$

where $J(\boldsymbol{\eta})$ is a state dependent transformation matrix of the form

$$J(\boldsymbol{\eta}) = J(\psi) = \begin{bmatrix} \cos(\psi) & -\sin(\psi) & 0 \\ \sin(\psi) & \cos(\psi) & 0 \\ 0 & 0 & 1 \end{bmatrix}$$

Notice that $J(\psi)$ is non-singular for all $\psi$ and that $J^{-1}(\psi) = J^T(\psi)$

## 2.2 Low frequency ship model

At low speed the low frequency motion of a large class of vessels can be described by the following model

$$M\dot{\boldsymbol{\nu}} + D\boldsymbol{\nu} = \boldsymbol{\tau} + J^T(\boldsymbol{\eta})\boldsymbol{b}$$

Here $\boldsymbol{\tau} \in \mathbb{R}^3$ is a vector containing the control forces and moments and $\boldsymbol{b} \in \mathbb{R}^3$ represents all unmodeled forces and moments due to wind, current and waves. The inertia matrix $M \in \mathbb{R}^{3\times 3}$ is assumed to have the form

$$M = \begin{bmatrix} m - X_{\dot{u}} & 0 & 0 \\ 0 & m - Y_{\dot{v}} & mx_G - Y_{\dot{r}} \\ 0 & mx_G - N_{\dot{v}} & I_z - N_{\dot{r}} \end{bmatrix}$$

where $m$ is the vessel mass, $I_z$ is the moment of inertia about the vessel-fixed $z$-axis and $x_G$ is the distance between the center of gravity and the origin of the vessel-fixed frame. $X_{\dot{u}}$, $Y_{\dot{v}}$, $Y_{\dot{r}}$, $N_{\dot{v}}$ and $N_{\dot{r}}$ are added mass and inertia terms. Finally, the linear damping matrix $D \in \mathbb{R}^{3\times 3}$ is defined as

$$D = \begin{bmatrix} -X_u & 0 & 0 \\ 0 & -Y_v & mu_0 - Y_r \\ 0 & -N_v & mx_G u_0 - N_r \end{bmatrix}$$

where the cruise speed $u_0 = 0$ in DP and $u_0 > 0$ when moving forward. Generally, the damping forces will be nonlinear, however for DP and cruising at low constant speed linear damping is a good assumption.

## 2.3 First-order wave-induced model

Generally, a linear wave frequency model of order $p$ can be expressed as

$$\begin{aligned} \dot{\boldsymbol{\xi}} &= \Omega_p \boldsymbol{\xi} + \Sigma_p \boldsymbol{w}_{\boldsymbol{\xi}} \\ \boldsymbol{\eta}_w &= \Gamma_p \boldsymbol{\xi} \end{aligned}$$

where $\boldsymbol{\xi} \in \mathbb{R}^{3p}$, $\boldsymbol{w} = \begin{bmatrix} w_{w1} & w_{w2} & w_{w3} \end{bmatrix}^T$ is a zero-mean Gaussian white noise process and $\Omega_p$, $\Sigma_p$ and $\Gamma_p$ are constant matrices of appropriate sizes. The vector $\boldsymbol{\eta}_w = \begin{bmatrix} x_w & y_w & \psi_w \end{bmatrix}^T$ represents the first-order induced motion of the vessel. The sum of $\boldsymbol{\eta}_w$ and $\boldsymbol{\eta}$ gives the total ship motion. Here, the first-order wave-induced motions are approximated by a second-order wave model, yielding

$$\begin{aligned} \begin{bmatrix} \dot{\boldsymbol{\xi}}_1 \\ \dot{\boldsymbol{\xi}}_2 \end{bmatrix} &= \begin{bmatrix} 0 & I \\ -\Omega^2 & -2Z\Omega \end{bmatrix} \begin{bmatrix} \boldsymbol{\xi}_1 \\ \boldsymbol{\xi}_2 \end{bmatrix} + \begin{bmatrix} 0 \\ \Sigma \end{bmatrix} \boldsymbol{w}_{\boldsymbol{\xi}} \\ \boldsymbol{\eta}_w &= \begin{bmatrix} 0 & I \end{bmatrix} \begin{bmatrix} \boldsymbol{\xi}_1 \\ \boldsymbol{\xi}_2 \end{bmatrix} \end{aligned}$$

where

$$\begin{aligned} \boldsymbol{\xi}_i &= \begin{bmatrix} \xi_i^{(1)} & \xi_i^{(2)} & \xi_i^{(3)} \end{bmatrix}^T, \quad i = 1, 2 \\ \Omega &= diag\{\omega_{01}, \omega_{02}, \omega_{03}\} \\ Z &= diag\{\zeta_1, \zeta_2, \zeta_3\} \\ \Sigma &= diag\{\sigma_1, \sigma_2, \sigma_3\} \end{aligned}$$

Compactly written

$$\begin{aligned} \dot{\boldsymbol{\xi}} &= \Omega_2 \boldsymbol{\xi} + \Sigma_2 \boldsymbol{w}_{\boldsymbol{\xi}} \\ \boldsymbol{\eta}_w &= \Gamma_2 \boldsymbol{\xi} \end{aligned}$$

## 2.4 Slowly-varying Environmental Disturbances

The forces and moment due to wind, currents and waves are assumed to be slowly varying. The model used here is the first-order Markov process

$$\dot{\boldsymbol{b}} = -T\boldsymbol{b} + \Psi \boldsymbol{n}$$

where $\boldsymbol{b} \in \mathbb{R}^3$ is the vector representation of the slowly varying forces and moment, $\boldsymbol{n} \in \mathbb{R}^3$ is a vector of zero-mean Gaussian white noise, $T \in \mathbb{R}^{3\times3}$ is a diagonal matrix of positive time constants and $\Psi \in \mathbb{R}^{3\times3}$ is a diagonal matrix scaling the amplitude of $\boldsymbol{n}$.

## 2.5 Total system

It is assumed that only position and heading measurements are available, leading to

$$\boldsymbol{y} = \boldsymbol{\eta} + \boldsymbol{\eta}_w + \boldsymbol{v}$$

Thus, the measurements are superpositions of the low frequency and high frequency motions and zero-mean Gaussian measurement noise $\boldsymbol{v}$. This leads to the total system

$$\begin{aligned} \dot{\boldsymbol{\eta}} &= J(\boldsymbol{\eta})\boldsymbol{\nu} \\ M\dot{\boldsymbol{\nu}} &= -D\boldsymbol{\nu} + J^T(\boldsymbol{\eta})\boldsymbol{b} + \boldsymbol{\tau} \\ \dot{\boldsymbol{b}} &= -T\boldsymbol{b} + \Psi\boldsymbol{n} \\ \dot{\boldsymbol{\xi}} &= \Omega_2\boldsymbol{\xi} + \Sigma_2\boldsymbol{w}_{\boldsymbol{\xi}} \\ \boldsymbol{y} &= \boldsymbol{\eta} + \boldsymbol{\eta}_w + \boldsymbol{v} = \boldsymbol{\eta} + \Gamma_2\boldsymbol{\xi} + \boldsymbol{v} \end{aligned}$$

Compactly written

$$\dot{\boldsymbol{x}} = A(\boldsymbol{x})\boldsymbol{x} + B\boldsymbol{\tau} + E\boldsymbol{w} \quad (1)$$
$$\boldsymbol{y} = C\boldsymbol{x} + \boldsymbol{v} \quad (2)$$

where

$$\boldsymbol{x} = \begin{bmatrix} \boldsymbol{\eta} \\ \boldsymbol{\nu} \\ \boldsymbol{b} \\ \boldsymbol{\xi} \end{bmatrix}, \qquad A(\boldsymbol{x}) = \begin{bmatrix} 0 & J(\boldsymbol{\eta}) & 0 & 0 \\ 0 & -M^{-1}D & M^{-1}J^T(\boldsymbol{\eta}) & 0 \\ 0 & 0 & -T & 0 \\ 0 & 0 & 0 & \Omega_2 \end{bmatrix}$$

$$B = \begin{bmatrix} 0 \\ M^{-1} \\ 0 \\ 0 \end{bmatrix}, \qquad C = \begin{bmatrix} I & 0 & 0 & \Gamma_2 \end{bmatrix}$$

$$\boldsymbol{w} = \begin{bmatrix} \boldsymbol{n} \\ \boldsymbol{w_\xi} \end{bmatrix}, \qquad E = \begin{bmatrix} 0 & 0 \\ 0 & 0 \\ \Psi & 0 \\ 0 & \Sigma_2 \end{bmatrix}$$

## 3 Observer design

The new observer design approach introduced in this paper is based on the theoretical results of [7], leading to a suboptimal observer as in [1] when applied to the model presented above. The first part of this section will be dedicated to the derivation of the theoretical observer, in the second part the suboptimal observer will be considered.

### 3.1 Nonlinear observer

In optimal control design (see [6] for more details) the optimal control $\boldsymbol{u}$ for a nonlinear system

$$\dot{\boldsymbol{x}} = \boldsymbol{f}(\boldsymbol{x}, \boldsymbol{u}, t) \quad (3)$$

with performance indicator

$$J(\boldsymbol{x}(t_0), \boldsymbol{u}, t_0) = \phi(\boldsymbol{x}(T), T) + \int_{t_0}^{T} L(\boldsymbol{x}, \boldsymbol{u}, t)dt \quad (4)$$

is given by the Hamilton-Jacobi-Bellman equation

$$-\frac{\partial J^*}{\partial t} = \min_u(H(\boldsymbol{x}, \boldsymbol{u}, J^*_{\boldsymbol{x}}, t))$$

where $J^*(\boldsymbol{x}(t_0), t_0) = \min_{\boldsymbol{u}} J(\boldsymbol{x}(t_0), \boldsymbol{u}, t_0)$ denotes the optimal cost and the Hamiltonian is defined by

$$H(\boldsymbol{x}, \boldsymbol{u}, \boldsymbol{\lambda}, t) = L(\boldsymbol{x}, \boldsymbol{u}, t) + \boldsymbol{\lambda}^T \boldsymbol{f}(\boldsymbol{x}, \boldsymbol{u}, t)$$

Considering a linear system with quadratic performance indicator leads to the linear-quadratic optimal control problem [6]. As the optimal control design problem is the dual of the optimal observer design problem and the dual of linear-quadratic optimal control is thus the Kalman observer [5], with a similar derivation as for the optimal control problem (3)-(4) a nonlinear optimal observer can

be constructed. The remaining section will be devoted to the derivation of this observer, inspired by the results of [7]. Consider to this end the system

$$\dot{\boldsymbol{x}} = \boldsymbol{f}(\boldsymbol{x}, \boldsymbol{w}, t) \quad (5)$$
$$\boldsymbol{y} = \boldsymbol{g}(\boldsymbol{x}, \boldsymbol{v}) \quad (6)$$

where $\boldsymbol{w}$ and $\boldsymbol{v}$ represent unmodeled forces and disturbances of the system dynamics and measurements. The performance indicator is defined as

$$J(\boldsymbol{x}, \boldsymbol{w}, t) = \phi(\boldsymbol{x}(t_0), t_0) + \int_{t_0}^{t} L(\boldsymbol{x}, \boldsymbol{w}, \tau) d\tau \quad (7)$$

with $L(\boldsymbol{x}, \boldsymbol{w}, \tau) \geq 0$. A typical example is $L = \frac{1}{2}(\boldsymbol{y} - \hat{\boldsymbol{y}})^T R(\boldsymbol{y} - \hat{\boldsymbol{y}}) + \frac{1}{2}\boldsymbol{w}^T Q \boldsymbol{w}$, where $\boldsymbol{y}$ is the measurement vector, $\hat{\boldsymbol{y}}$ is the measurement estimate and $R$ and $Q$ are positive definite weighting matrices.
The objective is to find an estimate of the state $\hat{\boldsymbol{x}}$ minimizing the criterion (7) and obeying the system dynamics (5) and measurements (6). For this purpose the following Hamiltonian function is defined

$$H(\boldsymbol{x}, \boldsymbol{w}, \boldsymbol{\lambda}, t) = -L(\boldsymbol{x}, \boldsymbol{w}, t) + \boldsymbol{\lambda}^T \boldsymbol{f}(\boldsymbol{x}, \boldsymbol{w}, t) \quad (8)$$

leading to the Hamilton-Jacobi-Bellman equation (see [6] for derivations)

$$-\frac{\partial J^*}{\partial t} = \min_{\boldsymbol{w}}(H(\boldsymbol{x}, \boldsymbol{w}, J^*_{\boldsymbol{x}}, t)) \quad (9)$$

where $J^*(\boldsymbol{x}(t), t) = \min_{\boldsymbol{w}} J(\boldsymbol{x}(t), \boldsymbol{w}, t)$ denotes the optimal costs. Solving this equation yields the nonlinear optimal observer for general nonlinear systems. Note that when the system is linear

$$\dot{\boldsymbol{x}} = A\boldsymbol{x} + B\boldsymbol{w}$$
$$\boldsymbol{y} = C\boldsymbol{x}$$

with quadratic performance indicator

$$\begin{aligned} J(\boldsymbol{x}, \boldsymbol{u}, t) = & \frac{1}{2}(\boldsymbol{x}(t_0) - \hat{\boldsymbol{x}}(t_0))^T P^{-1}(\boldsymbol{x}(t_0) - \hat{\boldsymbol{x}}(t_0)) \\ & + \frac{1}{2}\int_{t_0}^{t}(\boldsymbol{y} - C\boldsymbol{x})^T R^{-1}(\boldsymbol{y} - C\boldsymbol{x}) d\tau + \frac{1}{2}\int_{t_0}^{t} \boldsymbol{w}^T Q^{-1} \boldsymbol{w} d\tau \end{aligned}$$

leads to the Kalman observer [5].

### 3.2 Derivation of nonlinear suboptimal observer

For most formulations no exact solution to the Hamilton-Jacobi-Bellman equation (9) is known. In this section a suboptimal nonlinear observer for the model in section 2 will be presented making real-time implementation possible. Consider to this end the autonomous system

$$\dot{\boldsymbol{x}} = A(\boldsymbol{x})\boldsymbol{x} \quad (10)$$

with output function

$$\boldsymbol{y} = C\boldsymbol{x} \quad (11)$$

A system of the form

$$\dot{\hat{\boldsymbol{x}}} = A(\hat{\boldsymbol{x}})\hat{\boldsymbol{x}} + \boldsymbol{\kappa}$$

is a state estimator for (10)-(11) if the error is asymptotically stable at the zero equilibrium [1]. The term $\boldsymbol{\kappa}$ can be seen as a correction term, compensating for differences between the real observations $\boldsymbol{y}$ and expected observations $C\hat{\boldsymbol{x}}$. The objective is now to find an estimator $\hat{\boldsymbol{x}}$ consistent with the measurements $\boldsymbol{y}$ and obeying the dynamics of the system as well as possible. This implies that $\hat{\boldsymbol{x}}$ should be chosen such that the measurement error $\boldsymbol{y} - C\hat{\boldsymbol{x}}$ and the error in the dynamics $\boldsymbol{\kappa}$ are minimal under a cost indicator. As noted in the previous section, the observer design problem is the dual of the control design problem. In [1, 8] this property is used to construct a suboptimal observer using state-dependent Riccati equation (SDRE) techniques. This approach leads to an observer for (10)-(11) of the following form [1]

$$\begin{aligned} \dot{\hat{\boldsymbol{x}}} &= A(\hat{\boldsymbol{x}})\hat{\boldsymbol{x}} + K(\hat{\boldsymbol{x}})(\boldsymbol{y} - C\hat{\boldsymbol{x}}) \\ K(\hat{\boldsymbol{x}}) &= P(\hat{\boldsymbol{x}})C^T R^{-1} \\ 0 &= P(\hat{\boldsymbol{x}})A^T(\hat{\boldsymbol{x}}) + A(\hat{\boldsymbol{x}})P(\hat{\boldsymbol{x}}) - P(\hat{\boldsymbol{x}})C^T R^{-1} C P(\hat{\boldsymbol{x}}) + Q \end{aligned}$$

where $R$ and $Q$ are weighting matrices.
Defining the error as

$$\boldsymbol{e}(t) = \boldsymbol{x}(t) - \hat{\boldsymbol{x}}(t)$$

leads to the error dynamics

$$\begin{aligned} \dot{\boldsymbol{e}} &= A(\boldsymbol{x})\boldsymbol{x} - A(\hat{\boldsymbol{x}})\hat{\boldsymbol{x}} - K(\hat{\boldsymbol{x}})(\boldsymbol{y} - C\hat{\boldsymbol{x}}) \\ &= A(\boldsymbol{x})\boldsymbol{x} - A(\hat{\boldsymbol{x}})\boldsymbol{x} + A(\hat{\boldsymbol{x}})\boldsymbol{x} - A(\hat{\boldsymbol{x}})\hat{\boldsymbol{x}} - K(\hat{\boldsymbol{x}})C(\boldsymbol{x} - \hat{\boldsymbol{x}}) \\ &= (A(\boldsymbol{x}) - A(\hat{\boldsymbol{x}}))\boldsymbol{x} + (A(\hat{\boldsymbol{x}}) - K(\hat{\boldsymbol{x}})C)\boldsymbol{e} \\ &= (A(\hat{\boldsymbol{x}}) - K(\hat{\boldsymbol{x}})C)\boldsymbol{e} + (A(\boldsymbol{x}) - A(\hat{\boldsymbol{x}}))\boldsymbol{x} \end{aligned}$$

Using the theory of [1] local asymptotic stability of the estimator can be proven and the region for which this property holds can be found. For more details, see [9].

## 4 Simulations

As the new observer will be compared to the observer proposed in [4, 11] the ship used for the simulations in [11] is considered. This gives the following matrices

$$\begin{aligned} M &= 10^9 \begin{bmatrix} 0.0070 & 0 & 0 \\ 0 & 0.0110 & -0.0130 \\ 0 & -0.0130 & 3.1930 \end{bmatrix} \\ D &= \begin{bmatrix} 200000 & 0 & 0 \\ 0 & 100000 & -700000 \\ 0 & -700000 & 63900000 \end{bmatrix} \end{aligned}$$

The matrix with time constants is chosen as $T = 0_{3\times 3}$ for stability reasons. It is assumed that there is enough data avialable for good estimation of the dominating wave frequencies $\omega_i$. Further, the damping factor is chosen as proposed in [11] to be $\zeta = 0.1$. The new observer will be tested for the following choice of the matrices $Q$ and $R$

$$\begin{aligned} Q &= \begin{bmatrix} 10^{-5} I_9 & 0 \\ 0 & I_6 \end{bmatrix} \\ R &= I_3 \end{aligned}$$

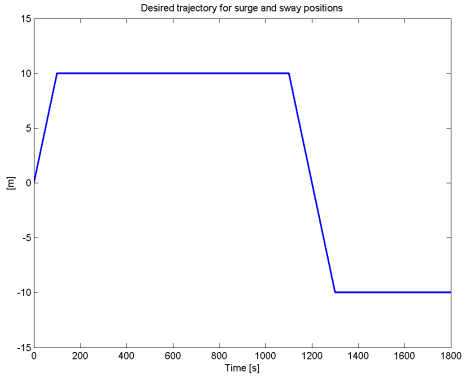


Figure 1: Desired trajectory of the vessel in surge and sway directions

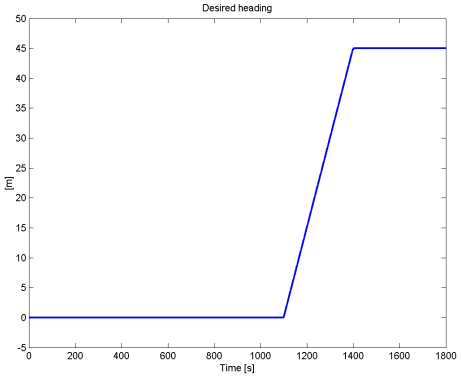


Figure 2: Desired heading of the vessel

The choice of the matrix $Q$ implies considerable uncertainty about the wave frequency model and high accuracy for both the low frequency model and the model used for the slowly-varying disturbances.
For the simulations MATLAB is used, solving the Riccati equation with the sign method, as implemented in [2]. The low frequency and high frequency displacements, $x_l$ and $x_h$ respectively, are generated separately, enabling comparison of the estimation errors of both methods. For the simulations the JONSWAP wave spectrum was used, with $H_s = 5m$, $T_p = 12s$ and $\gamma = 3.3$. The measurements $y$ are considered to be the superposition of the low frequency and high frequency displacements, thus $y = x_l + x_h$. For feedback control a PID controller was implemented with coefficients as in [11] using the estimated LF position of the vessel. The desired trajectory is illustrateed in Figures 1 and 2. In the represented simulation the vessel starts at position $(0, 0)$ with heading $0°$ and moves to position $(10, 10)$ in 100 seconds with constant rate of change and fixed heading at $0°$. After keeping this position and heading for 900 seconds the ship moves to position $(-10, -10)$ in 200 seconds and alters its heading to $45°$ in 300 seconds. This position and heading will be kept for the remaining simulation time.

## 5 Results

The test results show in all three degrees of freedom an improvement compared to the existing observer in both tracking and position keeping for this case. As the LF components of the displacement of the vessel are known due to the simulation implementation, comparison of the estimated and actual LF position is possible. Considering a sequence of $n$ estimations of the LF position $\{\hat{\boldsymbol{\eta}}^{(1)}, \ldots, \hat{\boldsymbol{\eta}}^{(n)}\}$ and their actual values $\{\boldsymbol{\eta}^{(1)}, \ldots, \boldsymbol{\eta}^{(n)}\}$ the norms

$$\frac{1}{n}\sum_{i=1}^{n} \|\hat{\boldsymbol{\eta}}_j^{(i)} - \boldsymbol{\eta}_j^{(i)}\|^2, \quad j = 1, 2, 3$$

indicate the deviation of the estimation error. This norm gives the following values for the considered simulation

| | SDRE | Existing |
|---|---|---|
| Surge | $6.3329 \cdot 10^{-2}$ | $3.9768 \cdot 10^{-2}$ |
| Sway | $1.5498 \cdot 10^{-1}$ | $6.3857 \cdot 10^{-2}$ |
| Yaw | $4.9448 \cdot 10^{-3}$ | $1.8719 \cdot 10^{-2}$ |

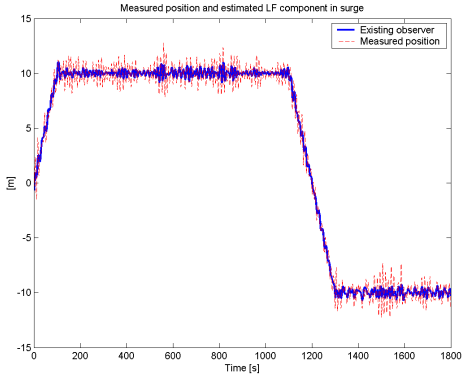


Figure 3: LF estimation using the existing observer and measured position in surge

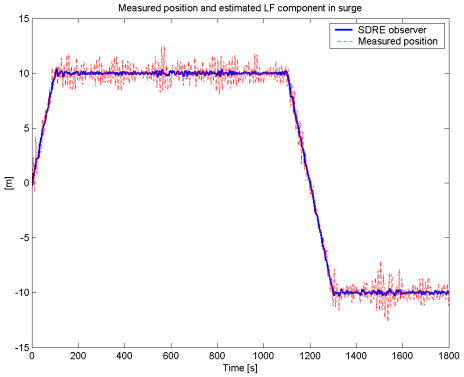


Figure 4: LF estimation using the SDRE observer and measured position in surge

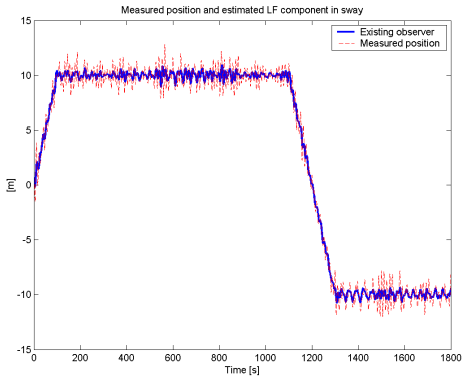


Figure 5: LF estimation using the existing observer and measured position in sway

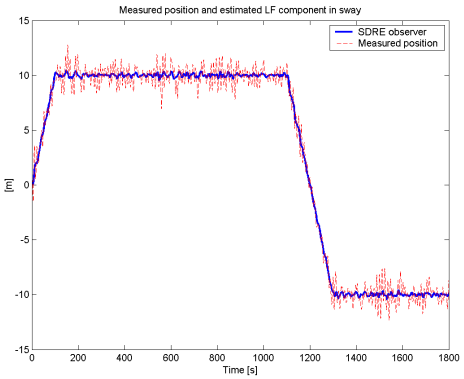


Figure 6: LF estimation using the SDRE observer and measured position in sway

The table shows that in surge and sway the estimations of the SDRE observer are less accurate than those of its existing counterpart, whereas in yaw the SDRE observer performs better than the existing observer. The smoother SDRE estimations in surge and sway seem contradictory to the less accurate norms when compared to the existing observer. This conflict can be explained considering the choice of the matrix $Q$ in the SDRE method. For the simulations $Q$ was tuned implying high accuracy for both the low frequency model and the model used for the slowly-varying disturbances and large uncertainty about the wave frequency model. With this assumption, differences between the measurements and the expected measurements, based on the estimations, are most likely to be of high frequency character. High frequency components in the LF motions are considered to be part of the wave frequency motions, leading to smoother estimations but loss of accuracy in estimation of the LF motions.

## 6 Conclusions

In this paper a new observer design approach was presented and a suboptimal observer was developed and compared to an existing observer. One of the advantages of the proposed approach is the

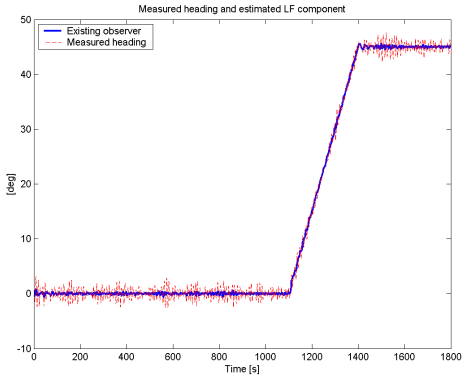


Figure 7: LF estimation using the existing observer and measured heading

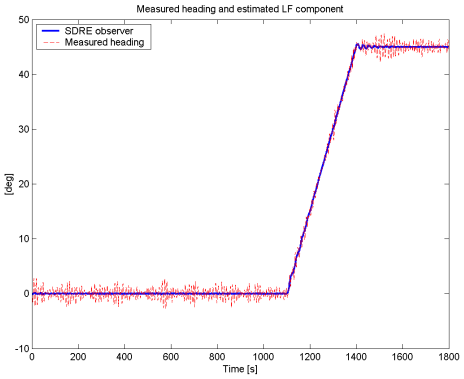


Figure 8: LF estimation using the SDRE observer and measured heading

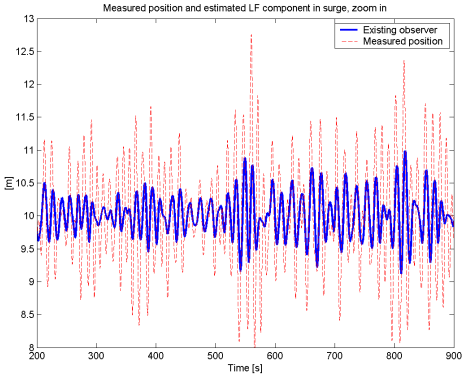


Figure 9: Zoom in on LF estimation and measured position in surge for the existing observer

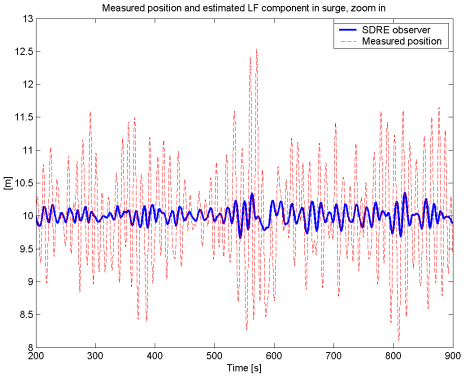


Figure 10: Zoom in on LF estimation and measured position in surge for the SDRE observer

flexibility it offers due to the fact that it is based on a general mathematical framework allowing the use of different models for ship motions. Drawback of the proposed approach is the loss of global asymptotic stability. However, for small errors in yaw angle estimation this property still holds locally for the new observer. Further, the advantages the SDRE approach offers in other areas of research make exploration of its possibilities for DP purposes attractive.
First tests show promising results in position estimation for station keeping and tracking in rough sea, however, more testing is necessary in order to provide more insight in the performance of the observer.
Further research on SDRE approach in observer design for dynamic positioning involves the usage of different models, derivation of tuning rules and exploration of its stability properties.

## References

[1] H. T. Banks, B. M. Lewis, and H. T. Tran. Nonlinear Feedback Controllers and Compensators: A State Dependent Riccati Equation Approach. Technical report, CRSC, 2003.

[2] B. N. Datta. *Numerical Methods for Linear Control Systems*. Elsevier Inc., 2004.

[3] T. I. Fossen. *Guidance and Control of Ocean Vehicles*. John Wiley & Sons Ltd., 1994.

[4] T. I. Fossen and J. P. Strand. Passive Nonlinear Observer Design for Ships Using Lyapunov Methods: Full-Scale Experimental Results with a Supply Vessel. *Automatica*, 35(1):3–16, 1999.

[5] A. H. Jazwinski. *Stochastic Processes and Filtering Theory*. Academic Press, Inc., 1970.

[6] F. L. Lewis and V. L. Syrmos. *Optimal Control*. John Wiley & Sons, Inc., 1995.

[7] W. Lohmiller and J. E. E. Slotine. Contraction Analysis of Nonlinear Distributed Systems. *International Journal of Control*, 78(9), 2005.

[8] C. P. Mracek, J. R. Cloutier, and C. A. D'Souza. A New Technique for Nonlinear Estimation. In *Proceedings of the IEEE Conference on Control Applications*, pages 338–343, 1996.

[9] J. G. Snijders. Wave Filtering and Thruster Allocation for Dynamic Positioned Ships. Master's thesis, Delft University of Technology, 2005. To appear.

[10] J. P. Strand and T. I. Fossen. Nonlinear Passive Observer for Ships with Adaptive Wave Filtering. In *New Directions in Nonlinear Observer Design*, pages 113–134. Springer-Verlag London Ltd., 1999.

[11] G. Torsetnes. Nonlinear Control and Observer Design for Dynamic Positioning using Contraction Theory. Master's thesis, Norwegian University of Science and Technology, 2004.

[12] G. Torsetnes, J. Jouffroy, and T. I. Fossen. Nonlinear Dynamic Positioning of Ships with Gain-Scheduled Wave Filtering. In *Proc. of the IEEE CDC'04*, 2004.